ORIGINAL ARTICLE

FGFR1 Cooperates with EGFR in Lung Cancer Oncogenesis, and Their Combined Inhibition Shows Improved Efficacy

Alvaro Quintanal-Villalonga, PhD,[a,b,c] Sonia Molina-Pinelo, PhD,[d,e] Cristina Cirauqui, PhD,[a,b] Laura Ojeda-Márquez, MSc,[a,b,e] Ángela Marrugal, MSc,[a,b] Rocío Suarez,[a,b] Esther Conde, PhD,[e,f] Santiago Ponce-Aix, MD,[e,g] Ana Belén Enguita, MD,[h] Amancio Carnero, PhD,[d,e] Irene Ferrer, PhD,[a,b,e,*] Luis Paz-Ares, MD, PhD[a,b,e,g,i]

[a]*H12O-CNIO Lung Cancer Clinical Research Unit, Biomedical Research Foundation i+12, Madrid, Spain*
[b]*H12O-CNIO Lung Cancer Clinical Research Unit, Spanish National Cancer Research Centre (CNIO), Madrid, Spain*
[c]*Program in Molecular Pharmacology, Memorial Sloan Kettering Cancer Center, New York, New York*
[d]*Insitute for Biomedical Research in Seville (UHVR, SNRC, Seville University), Seville, Spain*
[e]*CIBERONC, Madrid, Spain*
[f]*Therapeutic Targets Laboratory, University Hospital HM Sanchinarro, Madrid, Spain*
[g]*Medical Oncology Department, University Hospital Doce de Octubre Madrid, Spain*
[h]*Pathological Anatomy Department, University Hospital Doce de Octubre, Madrid, Spain*
[i]*Medical School, Complutense University, Madrid, Spain*

Received 6 July 2018; revised 23 November 2018; accepted 4 December 2018
Available online - 9 January 2019

ABSTRACT

Introduction: There is substantial evidence for the oncogenic effects of fibroblast growth factor receptor 1 (FGFR1) in many types of cancer, including lung cancer, but the role of this receptor has not been addressed specifically in lung adenocarcinoma.

Methods: We performed FGFR1 and EGFR overexpression and co-overexpression assays in adenocarcinoma and in inmortalized lung cell lines, and we also carried out surrogate and interaction assays. We performed monotherapy and combination EGFR/FGFR inhibitor sensitivity assays in vitro and in vivo in cell line– and patient-derived xenografts. We determined FGFR1 mRNA expression in a cohort of patients with anti–EGFR therapy–treated adenocarcinoma.

Results: We have reported a cooperative interaction between FGFR1 and EGFR in this context, resulting in increased EGFR activation and oncogenic signaling. We have provided in vitro and in vivo evidence indicating that FGFR1 expression increases tumorigenicity in cells with high EGFR activation in EGFR-mutated and EGFR wild-type models. At the clinical level, we have shown that high FGFR1 expression levels predict higher resistance to erlotinib or gefitinib in a cohort of patients with tyrosine kinase inhibitor–treated EGFR-mutated and EGFR wild-type lung adenocarcinoma. Dual EGFR and FGFR inhibition in FGFR1-overexpressing, EGFR-activated models shows synergistic effects on tumor growth in vitro and in cell line– and patient-derived xenografts, suggesting that patients with tumors bearing these characteristics may benefit from combined EGFR/FGFR inhibition.

Conclusion: These results support the extended the use of EGFR inhibitors beyond monotherapy in the EGFR-mutated adenocarcinoma setting in combination with FGFR inhibitors for selected patients with increased FGFR1 overexpression and EGFR activation.

***Corresponding author.**

Dr. Ferrer and Dr. Luis Paz-Ares equally contributed to this work.

Disclosure: Dr. Quintanal-Villalonga has patent P201730928 and patent PCT/ES2018/070502 pending. Dr. Molina-Pinelo has patent P201730928 and patent PCT/ES2018/070502 pending. Dr. Conde reports personal fees from Pfizer and Roche outside the submitted work. Dr. Carnero has patent P201730928 and patent PCT/ES2018/070502 pending. Dr. Paz-Ares reports personal fees from Roche, Lilly, MSD, BMS, AstraZeneca, Boehringer Ingrlhrim, Pfizer, Takeda, Novartis, Merck Serono, and Amgen outside the submitted work; in addition, Dr. Paz-Ares has patent P201730928 and patent PCT/ES2018/070502 pending. Dr. Ferrer has patent P201730928 and patent PCT/ES2018/070502 pending. The remaining authors declare no conflict of interest.

Address for correspondence: Irene Ferrer, PhD, H12O-CNIO Lung Cancer Clinical Research Unit Centro Nacional de Investigaciones Oncológicas (CNIO) Av. Melchor Fernández Almagro, 3 Madrid 28029, Spain. E-mail: iferrer@ext.cnio.es

ISSN: 1556-0864

https://doi.org/10.1016/j.jtho.2018.12.021

Keywords: FGFR1; EGFR; cooperation; combined inhibition

Introduction

Lung cancer is the leading cause of cancer-related deaths, being responsible for 27% of cancer mortality. Within lung cancer, adenocarcinoma represents the most prevalent histological type. Several driver alterations that are responsible for the initiation and progression of these tumors have been identified. Of these, one of the most relevant at the therapeutic level is mutation in the tyrosine kinase receptor EGFR, which is found in up to 20% of adenocarcinomas in white cohorts and in up to 30% to 50% of patients of Asiatic origin.[1,2] The discovery of these alterations and the development of EGFR inhibitors have significantly improved outcomes for such patients.[3] However, in spite of the benefits achieved by EGFR inhibition, tumor relapse is universal and there are patients whose tumors harbor unknown EGFR mutations or exhibit EGFR activation without mutations, thereby excluding them as candidates for these therapies.[4–6] The identification of predictive biomarkers for EGFR therapy and novel therapeutic approaches with higher efficacy for treatment of these tumors is therefore crucial.

Besides EGFR, other tyrosine kinase receptors are currently gaining attention as potential therapeutic targets. Included among these is the fibroblast growth factor receptor (FGFR) family, which is involved in the progression of a variety of cancers.[7–11] In lung cancer, fibroblast growth factor receptor 1 (FGFR1) has shown oncogenic properties in preclinical models of squamous cell carcinomas, in which amplification of the gene is frequently observed through the activation of relevant signaling pathways such as signal transducer and activator of transcription (STAT), AKT, and mitogen-activated protein kinase,[12–15] opening the door for potential therapeutic targeting in this histological type of lung cancer. However, even though the preclinical results of using FGFR inhibitors were promising, the efficacy of drugs targeting FGFR1 in clinical trials has so far been discrete in this tumor subtype.[16] For this reason, the current main patient selection criterion for use of these inhibitors, namely, fibroblast growth factor receptor 1 gene (*FGFR1*) amplification, which is also seen in 1% to 3% of lung adenocarcinomas,[17,18] is being questioned, and there is in fact evidence showing that FGFR1 mRNA and FGFR1 protein expression may be better predictors of FGFR inhibition efficacy.[19,20] In light of these results, current research on FGFR inhibition is focused on the identification of optimal predictive biomarkers.[21] Furthermore, there may be a cooperative interaction between EGFR and FGFR1 in lung adenocarcinomas, as FGFR1 upregulation has been reported as a mechanism of resistance to EGFR-targeted therapy.[22–24] In this work, we have aimed to study the biological interactions between both signaling pathways and the potential therapeutic implications of their inhibition.

Materials and Methods

Cell Lines

Characteristics of the cell lines used are shown in Supplementary Table 1. All cell lines were grown in accordance with the American Type Culture Collection indications and were authenticated and regularly tested for *Mycoplasma*.

Transfections

Cell lines were transfected with TransIT-X2 (Mirus, Madison, WI). FGFR1 (RC202080) complementary DNA clones were obtained from Origene (Rockville, MD) in the pCMV6 plasmid (PS100001). Wild-type EGFR and EGFR L858R/T790M in the pBABE plasmid, as well as the empty pBABE plasmid were obtained from Addgene (Cambridge, MA).

Growth Factor Stimulation

Cells were cultured in fetal bovine serum–free medium for 5 hours to induce basal phosphorylation levels and then stimulated with serum-free medium containing fibroblast growth factor 1 (50 ng/mL [Immunostep, Orsay, France]), epidermal growth factor (EGF) (50 ng/mL [Immunostep]), or complete medium (10% fetal bovine serum) for 15 minutes. Protein extracts were subsequently obtained as indicated later in this article.

Surrogated Assays

Surrogated assays were performed as indicated in Guijarro et al.[25] For growth curves, multiple 12-well plates were seeded with 10,000 cells/well and fixed every 2 days. Cell proliferation was determined by crystal violet staining normalized to the day 0 plate. For clonability and soft agar assays, the number of colonies was counted after a period of 2 weeks to 1 month after seeding. A minimum of three biological replicates (independent experiments) were performed for each assay. For each biological replicate, three technical replicates per condition were carried out.

Coimmunolocalization

Anti-EGFR (Thermo Fisher Scientific, Waltham, MA) and anti-FGFR1 (Cell Signaling Technology, Danvers, MA)

primary antibodies and Alexa Fluor 488 (Thermo Fisher Scientific) and Alexa Fluor 555 secondary antibodies (Thermo Fisher Scientific) were used under the conditions suggested by the manufacturer. Photographs of 15 to 20 cells per condition were taken with an SP5-WLL confocal microscope (Leica Microsystems, Wetzlar, Germany).

Cell Line Treatments

The concentration required to inhibit cell growth by 50% (GI_{50}) was calculated as in Moneo et al.[26] For combination treatments, the GI_{50} values of the EGFR inhibitors were calculated in the presence of the approximate mean value of the IC20 FGFR-inhibitor concentration and the double of this concentration value. The synergism between both kind of inhibitors was calculated as by Chou.[27] To study treatments' effects on downstream signaling, cells were treated for 24 hours with the erlotinib GI_{50} alone or in combination with the GI_{50} of AZD4547, and protein extraction was performed.

PDXs

We have used a collection of patient-derived xenograft (PDX) models that were constructed on the basis of patients with NSCLC and established by our group at the Institute of Biomedicine in Seville. Early-stage resected lung tumors from patients from Hospital Universitario Virgen del Rocío in Seville, Spain, were obtained through the hospital biobank and inoculated subcutaneously and expanded in successive groups of nude mice. For this study, PDXs were selected depending on their histological type, genetic background, and FGFR1 expression and EGFR activation. We have used three models: TP103 (EGFR and p53 mutated), TP57, and TP126 (KRAS and p53 mutated). Mutational profile was determined by the OncoNIM Seq Lung Panel, and the specific mutation frequency was determined by digital droplet polymerase chain reaction. The human samples were stored at the Hospital Universitario Virgen del Rocío Biobank after written informed consent forms were signed by all patients.

Cell Line and PDXs and In Vivo Treatments

For cell line xenografts, 2×10^6 cells in phosphate-buffered saline/Matrigel (1:1) were injected into female 6-week-old athymic nude mice. For the PDXs, previously amplified tumors were cut into 50- to 100-mm^3 pieces, and each was inserted subcutaneously into one flank of the mouse. Four mice were included in the control groups and six mice were included in the experimental groups on the basis of previous work in the laboratory. Tumors were measured twice a week, and when tumor volume had reached 150 to 200 mm^3, the mice were randomized into groups with similar mean tumor sizes and SDs. Mouse weights were measured once a week to monitor toxicity. Mice were humanely killed at the end of treatment and tumors harvested. Erlotinib, AZD4547, or their combination was administered 5 times a week, at a dose of 50 mg of erlotinib/kg/d for the erlotinib-resistant models and a dose of 25 mg erlotinib/kg/d for the erlotinib-sensitive models. AZD4547 was administered at a concentration of 5 mg/kg/d. The same therapeutic schedule was used for the osimertinib treatments but with a dose of 10 mg/kg/d. All drugs were administered by oral gavage. The duration of the treatments was 5 weeks unless rapid tumor growth necessitated an earlier end point. In these experiments, blinding was achieved by having one person treat the animals and a different person measure the tumors and processing the data.

Immunoblot

Western blot was performed as indicated by Ferrer et al.[28] with use of the following antibodies: FGFR1 (Cell Signaling Technology), pFGFR1 (Millipore, Bedford, MA), AKT (Cell Signaling Technology), phosphorylated AKT (pAKT) (Cell Signaling Technology), p42/p44 (Cell Signaling Technology), p-p42/p44 (Cell Signaling Technology), signal transducer and activator of transcription 3 (STAT3) (Cell Signaling Technology), phosphorylated STAT3 (pSTAT3) (Cell Signaling Technology), α-tubulin (Sigma, St. Louis, MO), β-actin (Sigma), EGFR (Cell Signaling Technology), and phosphorylated EGFR (pEGFR) (Cell Signaling Technology). Western blot images with a high number of lanes were assembled from blots run in parallel and with a common reference sample on both gels.

Coimmunoprecipitation

Coimmunoprecipitation was performed by using the EZ View Red Protein G Affinity Gel (Sigma). Protein extracts were made in HEPES 50 mM, NaCl 150 mM, and *n*-octylglucoside 1% and supplemented with a protease inhibitor cocktail (cOmpleteMini, Roche, Indianapolis, IN) and a phosphatase inhibitor cocktail (PhosSTOP, Roche). Next, 2-mg protein aliquots were precleared and incubated with the antibody-conjugated beads. The EGFR antibody (Cell Signaling Technology) was used in a 1:100 dilution for the immunoprecipitation, and an equal amount of anti–immunoglobulin G isotype control antibody (Cell Signaling Technology) was used as a negative control. Immunocomplexes were denatured by boiling in Laemmli buffer, and a Western blot protocol was performed to confirm the immunoprecipitation and assess the coimmunoprecipitation of FGFR1.

RNA Extraction and Analysis

RNA extraction of paraffin-embedded patient tumor tissues was performed with the RecoverAll Extraction Kit

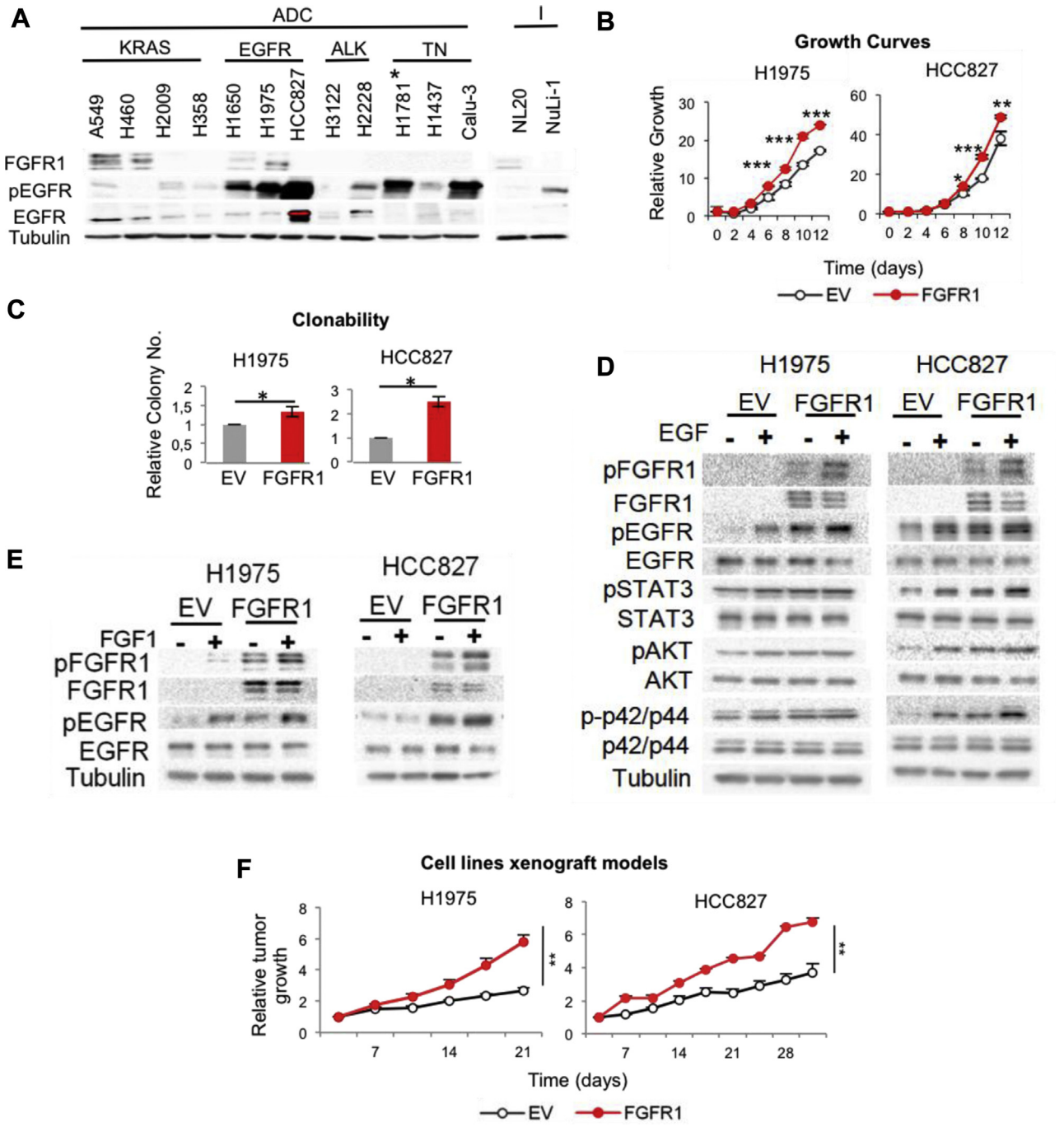

Figure 1. Effect of fibroblast growth factor receptor 1 (FGFR1) overexpression on tumorigenesis of EGFR mutation-driven lung adenocarcinoma cell lines. (*A*) Characterization of FGFR1 and EGFR protein expression and EGFR activation in a panel of lung cell lines. (*B*) Growth curves in 10% fetal bovine serum and (*C*) clonability assays of FGFR1-overexpressing EGFR-mutated adenocarcinoma cell lines. (*D*) Western blotting of the activation of the EGFR and receptor tyrosine kinase-related signaling pathways in the FGFR1-overexpressing, EGFR-mutated H1975 and HCC827 lung adenocarcinoma cell lines compared with that in the empty vector (EV)-containing cell lines after stimulation with recombinant human epidermal growth factor. (*E*) Western blotting of the activation of the EGFR and receptor tyrosine kinase-related signaling pathways in FGFR1-overexpressing H1975 and HCC827 cells after stimulation with the fibroblast growth factor receptor-specific fibroblast growth factor 1. (*F*) Growth assessment of the tumors generated by FGFR1-overexpressing H1975 and HCC827 cell lines. Four and five mice were included in the EV and FGFR1 groups, respectively. The colony number is shown for the clonability assays. All the values were normalized to the EV control, and the mean of all the normalized replicates is presented. For Western blotting, cells were serum-starved for 5 hours before protein extraction. For the growth factor-stimulated conditions, serum-starved cells were stimulated with serum-free medium containing FGF1 15 minutes before protein extraction. All experiments were reproduced a minimum of three times in the laboratory. For growth curves and Western blots, a representative figure/image is shown. On the growth curves, the means and SDs for the technical replicates are shown. *p* Values were

(Life Technologies, Grand Island, NY). RNA samples were reverse transcribed with the TaqMan Reverse Transcription Kit (Life Technologies). Gene expression was analyzed after a preamplification step performed with the TaqMan Preamp Master Mix Kit (Applied Biosystems, Foster City, CA) by using two TaqMan probes from Life Technologies: Hs00917379_m1 FAM (FGFR1) and Hs99999907_m1 FAM (beta-2-microglobulin [B2M]). B2M expression was used to normalize the expression data.

Information on sensitivity to EGFR inhibitors lapatinib and erlotinib and of FGFR1 mRNA expression was obtained from the Cancer Cell Line Encyclopedia database (https://portals.broadinstitute.org/ccle/home), which is a public database of cancer cell lines' sensitivity to EGFR inhibitors.

Clinical Samples

The present study involved a cohort of 87 subjects in whom advanced (stage IIIC–IV) NSCLC had been diagnosed at the University Hospital 12 de Octubre (Madrid, Spain) and who had been given erlotinib or gefitinib as their or a further line of treatment. Tumor samples were sent to a pathology laboratory for diagnosis and prepared for storage by formalin fixation and paraffin embedding. The inclusion criteria were (1) a confirmed diagnosis of NSCLC, (2) access to patient clinical information, and (3) availability of tumor tissue obtained by surgical resection. For the tumor marker prognostic study, the Reporting Recommendations for Tumor Marker Prognostic Study[29] reporting guidelines were followed. Baseline characteristics of the patient cohorts are summarized in Supplementary Table 2.

Study Approval

Written informed consent was provided by all patients. The project was approved by the research ethics committee of the Hospital Universitario 12 Octubre (Madrid, Spain) (CEI 16/297). The procedures involving animals were approved by the animal protection committee of the Comunidad Autónoma de Madrid (Approval ID PROEX134/16).

Statistics

In vitro data are represented as the mean plus or minus SD to indicate variation within each group of data. Statistical analysis was performed with the SPSS statistical package (version 19, IBM Corporation, Armonk, NY). The in vitro and in vivo experiments were analyzed by using an unpaired nonparametric Mann-Whitney *U* or Student *t* tests. *p* Values less than 0.05 were considered significant. The Kaplan-Meier method was utilized for survival analyses of the clinical data and cell line xenograft experiments. Overall survival was defined as the length of time from the date of starting treatment to the date of death or last follow-up. Progression-free survival was defined as the length of time from the date of treatment initiation to the date of progression/death or last follow-up. A log-rank test was used to analyze differences in survival among groups. To obtain the hazard ratio (HR) values, the Cox proportional hazards model was used.

Results

First, we measured protein expression levels of FGFR1 and EGFR in adenocarcinoma cell lines with different genetic backgrounds and in two immortalized epithelial lung cell lines (see Supplementary Table 1). Relevant EGFR activation was observed in the EGFR-mutated cell lines, as expected, and in two other additional cell lines, Calu3 and H1781, without known EGFR mutations (Fig. 1*A*). EGFR mutational profiling in these two cell lines revealed no EGFR activating mutations in either cell line (data not shown). FGFR1 protein expression was detected in a few of the cell lines tested, but no relevant pFGFR1 was detected by Western blot (data not shown).

FGFR1 Cooperates with EGFR, Enhancing Its Tumorigenic Properties in Lung Adenocarcinoma Cell Lines

To study the role of FGFR1 in the context of EGFR-dependent lung adenocarcinoma, FGFR1 was overexpressed in adenocarcinoma cells with different EGFR mutations. FGFR1 overexpression in these cell lines (fold changes in FGFR1 expression of 15.2 and 24.7 for H1975 and HCC827, respectively) increased proliferation and clonability (Fig. 1*B* and *C*) relative to that in the control cell lines. Only one of these cell lines, HCC827, was able to form colonies in soft agar in our hands and produced a higher number of colonies that were also slightly bigger when FGFR1 was overexpressed (Supplementary Fig. 1*A*).

obtained with the two-sided Mann-Whitney *U* test and are indicated by asterisks (*$p < 0.05$, **$p < 0.01$, and ***$p < 0.001$). *In the H1781 cell line, referred to as EGFR wild-type in the literature (see Supplementary Table 1), the EGFR activating L858R mutation was detected. Because of the high number of cell lines analyzed, not fitting in a single gel, different gels were run in parallel with common internal reference samples, and the assembled images including all cell lines are shown. ADC, adenocarcinoma; ALK, ALK receptor tyrosine kinase translocation; I, immortalized; KRAS, KRAS mutated; EGFR, EGFR mutated; TN, triple negative (referring to the absence of KRAS, EGFR, and ALK alterations); FGFR1, FGFR1-overexpressing; pEGFR, phosphorylated EGFR; pFGFR1, phosphorylated fibroblast growth factor receptor 1; STAT3, signal transducer and activator of transcription 3; pSTAT3, phosphorylated signal transducer and activator of transcription 3; pAKT, phosphorylated AKT.

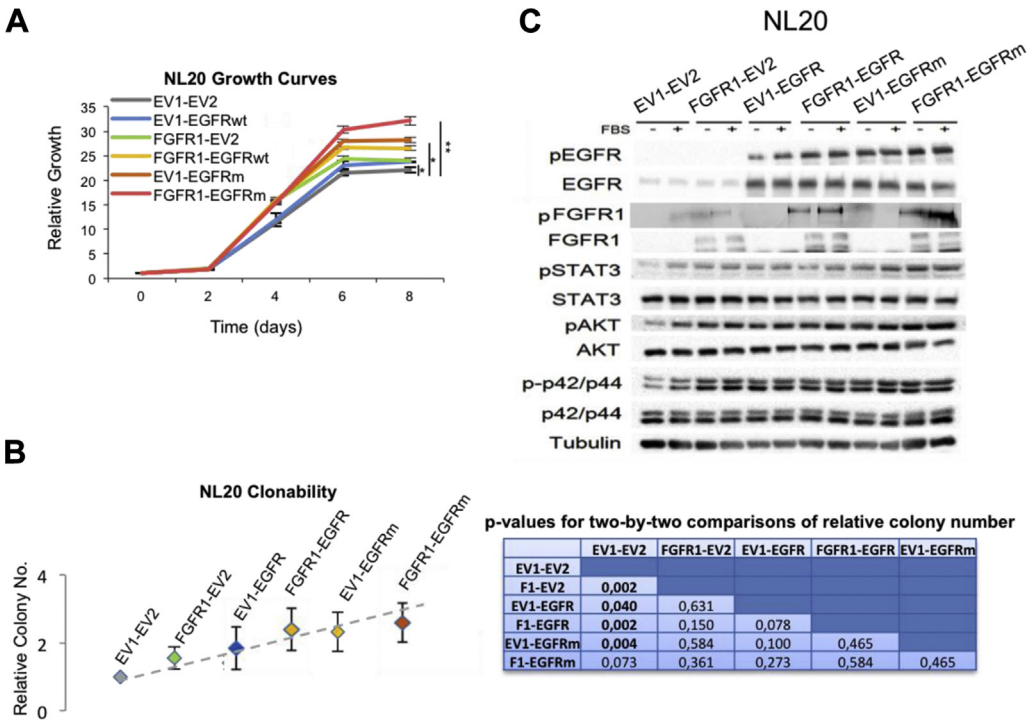

	EV1-EV2	FGFR1-EV2	EV1-EGFR	FGFR1-EGFR	EV1-EGFRm
EV1-EV2					
F1-EV2	0,002				
EV1-EGFR	0,040	0,631			
F1-EGFR	0,002	0,150	0,078		
EV1-EGFRm	0,004	0,584	0,100	0,465	
F1-EGFRm	0,073	0,361	0,273	0,584	0,465

Figure 2. Oncogenic cooperation of fibroblast growth factor receptor 1 (FGFR1) with mutated and wild-type activated EGFR. Growth curves in 10% fetal bovine serum (*A*) for NL20 cell lines overexpressing FGFR1 with or without coexpression of wild-type or EGFR L858R/T790M. (*B*) Clonability assays of the entire panel of NL20 cell lines generated. (*C*) Western blotting of proteins involved in the activation of fibroblast growth factor receptor–related signaling pathways in the FGFR1-EGFR interaction models after stimulation with fetal bovine serum in the NL20 cell line panel. For growth curves, a representative figure/image is shown. On the growth curves, the mean and SD for the technical replicates are shown. The colony number is shown for the clonability. All the values were normalized to the empty vector (EV) control, and the mean of all the normalized replicates is presented. For Western blots, a representative image is shown. *p* Values were obtained with the two-sided Mann-Whitney *U* test and are indicated by asterisks (*$p < 0.05$, **$p < 0.01$; and ***$p < 0.001$). EV1, empty vector 1; EV2, empty vector 2; F1, FGFR1; EGFRwt, wild type EGFR; EGFRm, mutant EGFR L858R/T790M; pEGFR, phosphorylated EGFR; pFGFR1, phosphorylated fibroblast growth factor receptor 1; pSTAT3, phosphorylated signal transducer and activator of transcription 3; STAT3, signal transducer and activator of transcription 3; pAKT, phosphorylated AKT.

We subsequently analyzed the activation of some signaling pathways related to EGFR and FGFRs in these cell lines. Under basal conditions, FGFR1 overexpression increased EGFR activation and slightly increased STAT3 and AKT signaling in H1975 and HCC827 cells. After EGF stimulation, pEGFR levels were higher in the FGFR1-overexpressing cell lines, and p42/p44 activation was also greater in FGFR1-overexpressing HCC827 cells

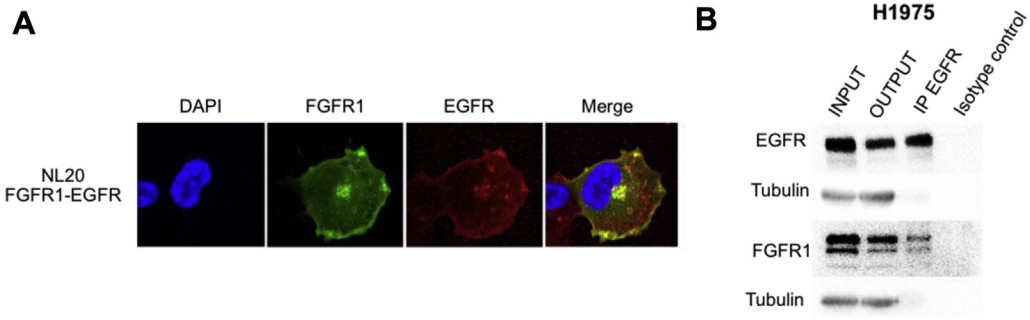

Figure 3. Interaction of EGFR with fibroblast growth factor receptor 1 (FGFR1). (*A*) Coimmunolocalization assays of EGFR and FGFR1 in the NL20 cell lines overexpressing wild-type EGFR and FGFR1. (*B*) Coimmunoprecipitation of EGFR with FGFR1 in the H1975 cell line. FGFR1 indicates FGFR1 overexpression, and EGFR indicates EGFR overexpression. A minimum of 15 independent images were captured in the immunofluorescence assays, and representative images for each condition are shown. The coimmunoprecipitation assays were independently reproduced three times and a representative blot is shown. INPUT, protein sample before immunoprecipitation; OUTPUT, protein sample after immunoprecipitation; DAPI, 4′,6-diamino-2-phenylindole; IP, immunoprecipitation.

than in the empty vector cell line. Interestingly, activation of the overexpressed FGFR was also increased by EGF stimulation (Fig. 1*D* and Supplementary Fig. 1*B*), suggesting a cooperation between EGFR and FGFR1. Complementarily, EGFR activation was promoted in FGFR1-overexpressing H1975 and HCC827 cells treated with the FGFR1-specific growth factor fibroblast growth factor 1 (Fig. 1*E* and Supplementary Fig. 1*C*). These results suggest that activation of either FGFR1 leads to increased EGFR signaling.

In addition, we xenografted the FGFR1-overexpressing H1975 and HCC827 cell lines into immunodeprived nude mice and monitored tumor growth. In these xenografts, FGFR1 overexpression increased tumor growth relative to that in the control xenografts (Fig. 1*F*).

The Cooperation between FGFR1 and EGFR Is not Specific to Constitutively Activated Forms of Mutant EGFR

To explore whether the cooperation between FGFR1 and EGFR is dependent on the presence of activating mutations in EGFR, different EGFR variants were overexpressed alone or in combination with FGFR1 in the immortalized epithelial lung cell line NL20 and surrogate assays were performed. Individual expression of FGFR1 or wild-type EGFR in the NL20 cell line increased proliferation to an extent similar to that the empty vector. When wild-type EGFR was coexpressed with FGFR1, the proliferation rate was significantly higher than under any of the previously mentioned conditions. Overexpression of the EGFR L858R/T790M variant alone increased proliferation compared with overexpression of wild-type EGFR. Finally, overexpression of FGFR1 in combination with EGFR L858R/T790M evoked the highest proliferation rate of all the cultures (Fig. 2*A*). In the clonability assay, increases in colony number were consistent with the reported effects on proliferation (Fig. 2*B*).

In general, overexpression of FGFR1 or wild-type EGFR increased the activation of the EGFR, STAT3, AKT, and p42/p44 signaling pathways, and this activation was further increased when wild-type EGFR was co-overexpressed with FGFR1. Overexpression of the constitutively active EGFR L858R/T790M mutant induced an even greater activation of these signaling pathways, and this effect was further enhanced by coexpressing mutant EGFR with FGFR1 (Fig. 2*C* and Supplementary Fig. 1*D*).

EGFR Physically Interacts with FGFR1

By immunofluorescence, we found that EGFR partially colocalized with FGFR1 in the cell membrane in the FGFR1-overexpressing, EGFR-overexpressing NL20 cell line (Fig. 3*A*). In addition, coimmunoprecipitation assays performed on a cell line with endogenous high levels of pEGFR and detectable FGFR1 expression (H1975) (see Fig. 1*A*) showed that FGFR1 coimmunoprecipitates with EGFR (Fig. 3*B*).

Combined EGFR and FGFR Inhibition Has Synergistic Effects In Vitro

Because of the aforementioned cooperation between EGFR and FGFR1, we tested the effects of the combined EGFR plus FGFR inhibition in the FGFR1-ovexpressing H1975 and HCC827 cell lines in vitro. We selected two EGFR inhibitors, erlotinib and osimertinib, and two selective FGFR inhibitors, AZD4547 and BGJ398. FGFR1 overexpression increased sensitivity to FGFR inhibitors and increased resistance to EGFR inhibitors compared with in the control cell lines (Fig. 4*A*). These effects were specific to the EGFR-dependent cell lines, as they were not reproduced in three different adenocarcinoma cell lines with no EGFR activation (Supplementary Fig. 1*E*). Consistently, high FGFR1 expression increased resistance to different EGFR inhibitors in lung adenocarcinoma and in NSCLC cell lines from a public database (Cancer Cell Line Encyclopedia) (Supplementary Fig. 2*A* and *B*). Furthermore, combined EGFR and FGFR inhibition exhibited synergy (Fig. 4*B*). As erlotinib combined with AZD4547 showed the strongest synergistic effect, this combination was chosen for further experiments.

Next, we determined the molecular effects of erlotinib and AZD4547 treatment, alone or in combination, in H1975 and HCC827 cell lines (Fig. 4*C*). In the FGFR1-overexpressing cell lines, although partial inhibition of pEGFR was achieved after erlotinib treatment, further abrogation of EGFR activation was reported after treatment with the combination of both inhibitors. Similar results were obtained for p42/p44 activation. Regarding the AKT signaling pathway, in the FGFR-overexpressing HCC827 cell line, the combination of both inhibitors decreased pAKT levels, as compared with when erlotinib was used alone, whereas no significant effects on this signaling pathway were reported for combination treatment in the H1975 cell line. Concerning the STAT3 signaling pathway, in the FGFR1-overexpressing H1975 cell line, the combination of both inhibitors showed a more pronounced reduction of pSTAT3 than with erlotinib monotherapy. Interestingly, in the HCC827 cell line, erlotinib treatment increased pSTAT3 activation. However, the addition of AZD4547 to erlotinib treatment of this cell line reduced this erlotinib-induced STAT3 activation. When the erlotinib-resistant H1975 cell line was treated with osimertinib and AZD4547 in monotherapy and in combination, the combination treatment showed

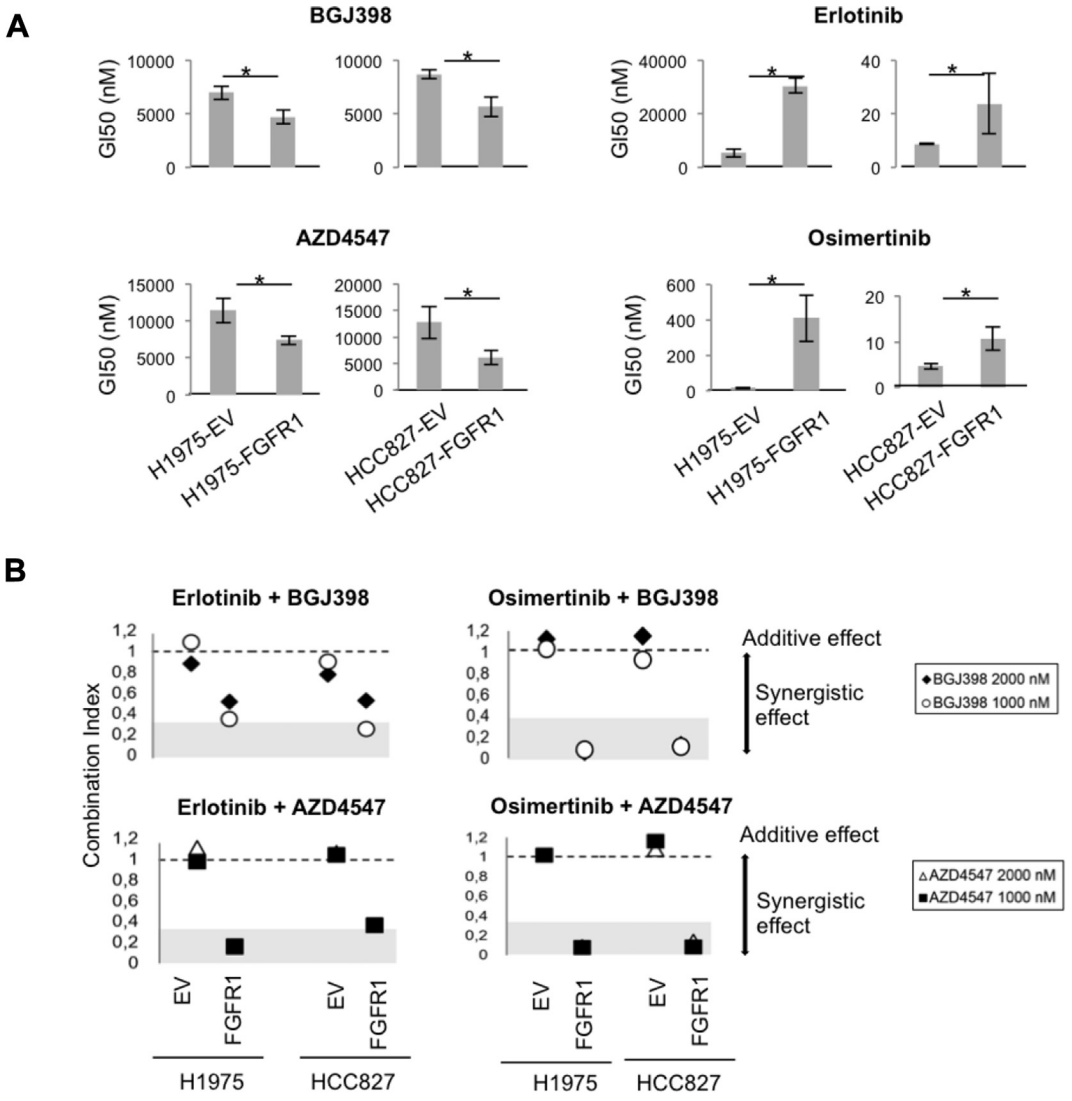
A
BGJ398
Erlotinib
AZD4547
Osimertinib
GI50 (nM)
H1975-EV
H1975-FGFR1
HCC827-EV
HCC827-FGFR1
B
Erlotinib + BGJ398
Osimertinib + BGJ398
Erlotinib + AZD4547
Osimertinib + AZD4547
Combination Index
Additive effect
Synergistic effect
BGJ398 2000 nM
BGJ398 1000 nM
AZD4547 2000 nM
AZD4547 1000 nM
EV
FGFR1
H1975
HCC827
C
H1975-EV
H1975-FGFR1
HCC827-EV
HCC827-FGFR1
AZD4547
Erlotinib
pFGFR1
FGFR1
pEGFR
EGFR
pSTAT3
STAT3
pAKT
AKT
p-p42/p44
p42/p44
Tubulin
D
H1975-EV
H1975-FGFR1
AZD4547
Osimertinib
pFGFR1
FGFR1
pEGFR
EGFR
pSTAT3
STAT3
pAKT
AKT
p-p42/p44
p42/p44
Tubulin

increased EGFR and mitogen-activated protein kinase signaling abrogation, as compared with when either monotherapy was used (Fig. 4*D*).

Dual Inhibition of EGFR and FGFR Is an Effective Therapeutic Approach for EGFR-Activated FGFR1/4-Expressing Tumors

We assessed the efficacy of combined erlotinib/AZD4547 treatment in vivo in EGFR-mutated xenograft models (H1975 and HCC827 cells). No toxicity was reported during these treatments (data not shown). In both models, FGFR1 overexpression resulted in higher sensitivity to FGFR inhibition, with a greater reduction in tumor growth after AZD4547 monotherapy than in the controls. This effect seemed to be FGFR specific, as FGFR inhibition did not significantly reduce tumor growth in the controls. Tumors generated by the H1975 cell line were intrinsically resistant to erlotinib treatment. However, combination of erlotinib with AZD4547 improved efficacy, especially in the FGFR1-overexpressing tumors. In the HCC827 xenografts, FGFR1 overexpression conferred increased resistance to EGFR inhibition, which was reversed by the combined treatment (Fig. 5*A* and *B*).

In terms of downstream signaling in the H1975 and HCC827 xenografts, AKT, p42/p44, and STAT3 signaling was increased in the tumors with FGFR1 overexpression relative to the increase in the controls, as was found in vitro. In both models, AZD4547 effectively reduced the activation of these signaling pathways only in the FGFR1-overexpressing xenografts. In the H1975 xenograft model, erlotinib caused only a slight decrease in pAKT and p-p42/p44 levels, which was enhanced by AZD4547 combination in the FGFR1-overexpressing xenografts. In the HCC827 xenografts, erlotinib treatment reduced AKT and p42/p44 activation, which was again further reduced by the combination therapy. As reported in vitro, erlotinib increased pSTAT3 levels in the HCC827 xenograft models, and only the combined treatment decreased STAT3 activation relative to that in the control (Fig 5*C* and Supplementary Fig. 2*C*).

Finally,we tested the effects of the combined therapy on three lung adenocarcinoma PDXs. First, we selected a model harboring EGFR L858R activating and T790M erlotinib resistance mutations (respective frequencies 31.2% and 17.4%) with high FGFR1 expression (TP103, Fig. 6*A*). In this model, erlotinib or AZD4547 monotherapy treatments modestly reduced tumor growth relative to that of the untreated tumors, and combination therapy showed higher efficacy (Fig. 6*B* and *C*). From a molecular standpoint, p-p42/p44 and pAKT levels were similarly reduced by erlotinib or AZD4547 monotherapy, and further reduction in the activation of these signaling pathways was achieved with combined therapy. In this model, erlotinib treatment also increased pSTAT3 levels, as compared with in the untreated control, and only the combination treatment could effectively reduce STAT3 activation (Fig. 6*D*).

As our previous in vitro and in vivo observations indicated that the EGFR-FGFR1 cooperation also takes place in the context of wild-type activated EGFR, we decided to test the efficacy of the erlotinib and AZD4547 treatments in two lung wild-type EGFR adenocarcinoma PDX models with high pEGFR and FGFR1 protein levels (TP57 and TP126, both KRAS mutated [see Fig. 6*A*]). In both models, erlotinib or AZD4547 monotherapy slightly reduced tumor growth relative to that in the untreated tumors, but their combination showed much stronger efficacy (see Fig. 6*B* and *C*). In line with these results, combined therapy inhibited EGFR, FGFR1, STAT3, p42/p44, and AKT to a greater extent than did either drug alone (Fig. 6*D*).

In addition, we tested the efficacy of combined AZD4547 and osimertinib treatment in the TP103 model, as osimertinib specifically targets the T790M EGFR mutation present in this PDX. This combination was not toxic (data not shown). Osimertinib treatment

Figure 4. In vitro effects of fibroblast growth factor receptor 1 (FGFR1) overexpression in EGFR and fibroblast growth factor receptor (FGFR) inhibitors' sensitivity. (*A*) Concentration required to inhibit cell growth by 50% (GI_{50}) assays of FGFR inhibitors BGJ398 and AZD4547 and EGFR inhibitors erlotinib and osimertinib in the H1975 and HCC827 cell lines, with or without overexpression of FGFR1. Nanomolar concentrations for all cell lines are shown. (*B*) Effects of the combination of EGFR- and FGFR-targeted therapies in these cell lines, assessed by the combinatory index (CI). Cell lines were treated with a fixed concentration of either FGFR inhibitor (1000 or 2000 nM) and a range of concentrations of either EGFR inhibitor to calculate the GI_{50} of the different EGFR-FGFR inhibitors combinations. The dashed line indicates the values (around $CI = 1$) at which combination therapy has an additive effect. Values under this line ($CI < 1$) reflect synergism. The gray area indicates the values showing strong synergism. (*C*) Effects of the combination of erlotinib and AZD4547 on protumorigenic signaling in these cell lines. (*D*) Effects of the combination of osimertinib and AZD4547 on protumorigenic signaling in the erlotinib-resistant H1975 cell line. Cells were treated with the GI_{50} concentration of either inhibitor for 24 hours before protein extraction. All experiments were reproduced a minimum of three times in the laboratory. In the GI_{50} assay results, the mean and SD for the technical replicates are shown. Protein extraction was performed after a 24-hour treatment with the GI_{50} of erlotinib and 2 μM of AZD4547. For Western blots, a representative image is shown. *p* Values were obtained with the two-sided Mann-Whitney *U* test and are indicated by asterisks ($^*p < 0.05$, $^{**}p < 0.01$, $^{***}p < 0.001$). EV, empty vector control; FGFR1, FGFR1-overexpressing; pFGFR1, phosphorylated fibroblast growth factor receptor 1; pEGFR, phosphorylated EGFR; pSTAT3, phosphorylated signal transducer and activator of transcription 3; STAT3, signal transducer and activator of transcription 3; pAKT, phosphorylated AKT.

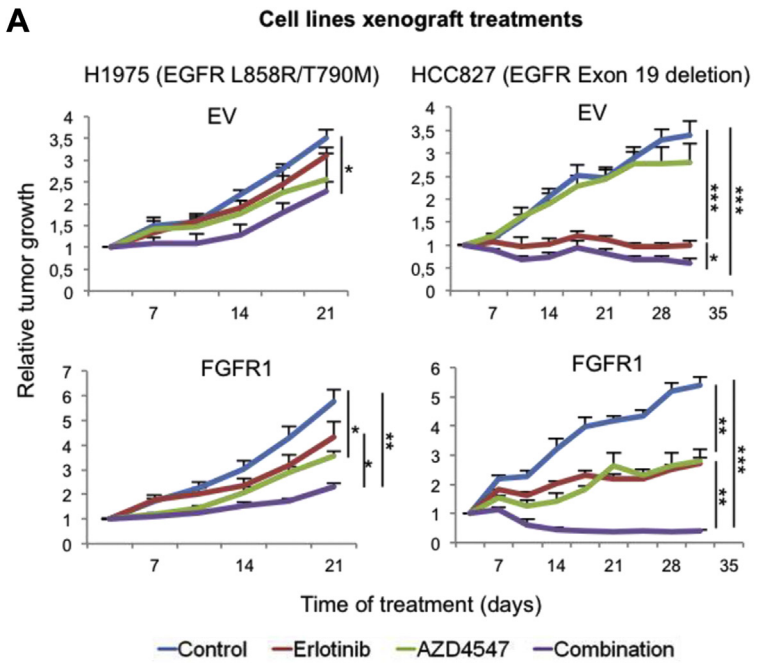

B

Model		Treatment	T/C (%)
H1975	EV	Erlotinib	92.1%
		AZD4547	99.6%
		Combination	67.3%
	FGFR1	Erlotinib	74.7%
		AZD4547	61.6%
		Combination	38.4%
HCC827	EV	Erlotinib	29.1%
		AZD4547	84.2%
		Combination	20.7%
	FGFR1	Erlotinib	48.2%
		AZD4547	50.8%
		Combination	7.2%

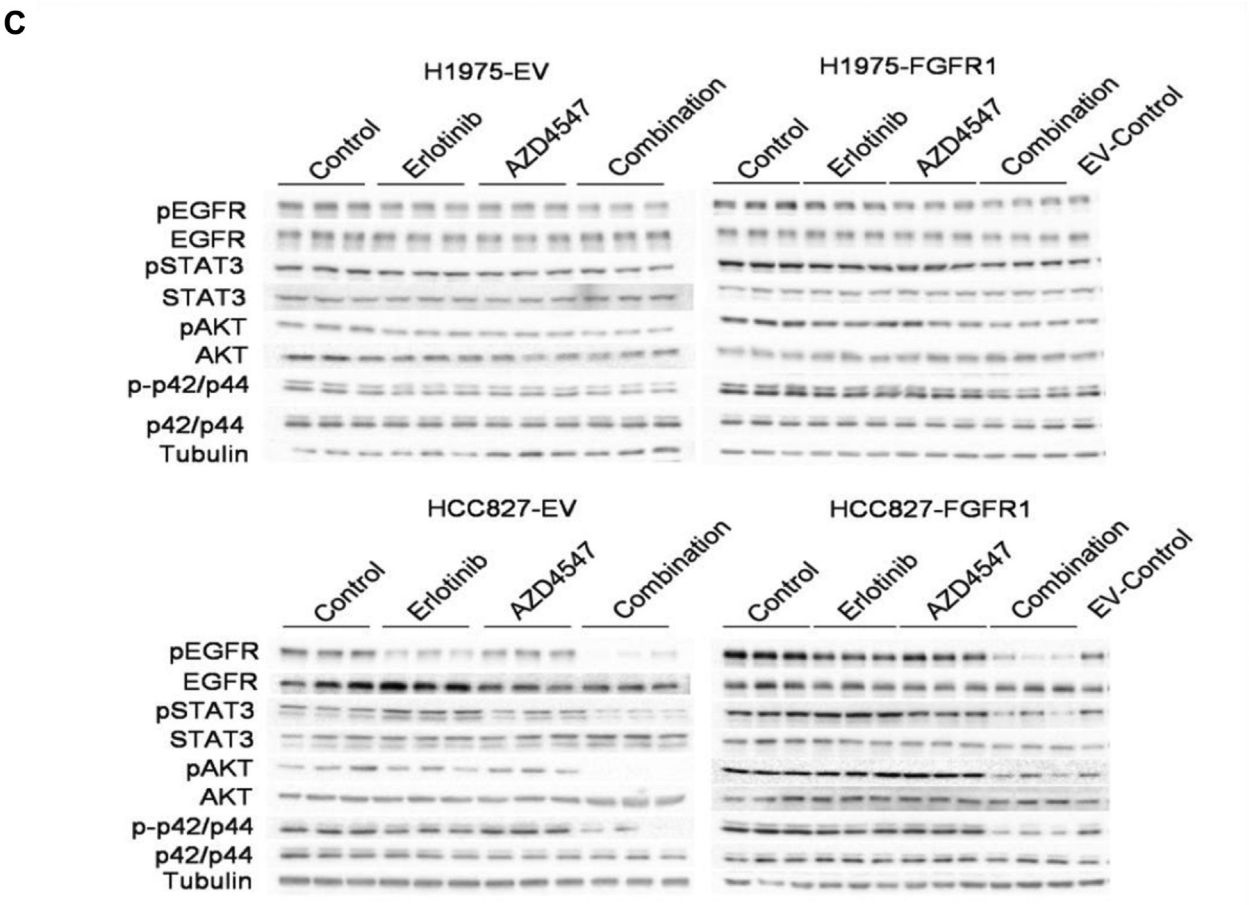

Figure 5. Effect of dual EGFR and fibroblast growth factor receptor inhibition in xenograft models. (*A*) Effect of erlotinib and AZD4547 on tumor growth of two EGFR-mutated adenocarcinoma cell line xenograft models, H1975 and HCC827, with or without fibroblast growth factor receptor 1 (FGFR1) overexpression. Relative tumor growth is shown, calculated as tumor volume increase from the beginning of the treatment. (*B*) Mean relative size of treated tumor groups compared with that of the untreated tumor control group (T/C), expressed as percentages. Two different erlotinib concentrations were used for these experiments: 50 mg/kg/d for the erlotinib-resistant models (H1975 xenograft) and 20 mg/kg/d for the

dramatically reduced tumor growth, but the combination regimen resulted in higher efficacy (Fig. 6*E* and *F*). Accordingly, the combined treatment more effectively inhibited FGFR1, EGFR, STAT3, p42/p44, and AKT than did either drug alone (Fig. 6*G*).

The Expression of FGFR1 Is a Potential Predictive Biomarker for Anti-EGFR Therapy Efficacy

FGFR1 mRNA expression was determined in formalin-fixed paraffin-embedded tumor samples from a cohort of patients with adenocarcinoma (including EGFR-mutated and EGFR wild-type tumors) treated with erlotinib or gefitinib with no prior anti-EGFR treatment (n = 47 [see Supplementary Table 2 and Fig. 6*H*]). We found that patients with high FGFR1 expression had a shorter progression-free period than the rest of the patients did (HR = 4.10, 95% confidence interval: 2.01–8.33, $p < 0.001$). In concondance with our previous results, these observations seemed to be independent of the presence of EGFR activating mutations, as similar results were obtained when only the EGFR-mutated or EGFR wild-type tumors were independently analyzed (Supplementary Fig. 3*A* and *B*). When we repeated these analyses in an extended cohort including patients with squamous and other NSCLC histological subtypes (n = 87 [see Supplementary Table 2]), we found the same effects (HR = 3.44, 95% confidence interval: 2.09–5.67, $p < 0.001$) for high FGFR1 expression (Supplementary Fig. 3*C*). We discarded the idea that these results were derived from a prognostic role of FGFR1 after analyzing The Cancer Genome Atlas lung cancer cohort, the patients of which were not known not receive an especific treatment targeting EGFR or FGFR (Supplementary Fig. 3*D*).

Discussion

We have shown here that FGFR1 cooperates with EGFR in EGFR-dependent lung adenocarcinoma through a reciprocal overactivation. Consistently, tumoral overexpression of FGFR1 determined decreased sensitivity to EGFR tyrosine kinase inhibitors in vitro and in vivo and conferred a poorer prognosis to patients treated with those inhibitors. Furthermore, we have provided in vitro (H1975 and HCC827) and in vivo (HCC827) evidence that the combination of EGFR and FGFR inhibition may be an effective therapy in EGFR-activated plus FGFR1-expressing lung adenocarcinoma tumors.

FGFR1 overexpression in EGFR-mutated models caused an increase in tumorigenicity in vivo and in vitro, which was accompanied by activation of EGFR and downstream signaling. We have also reproduced this FGFR-EGFR interaction in an immortalized lung cell line, confirming that the described cooperation is not exclusive to tumors with EGFR harboring activating mutations but also takes place in cells with overactivated wild-type EGFR.

EGFR was found to colocalize and coimmunoprecipitate with FGFR1, supporting a physical interaction between these molecules. Interestingly, pEGFR levels increased after stimulation with FGFR-specific ligands as phosphorylation of the FGFRs occurs after stimulation with EGF, thus providing biochemical evidence for EGFR-FGFR cooperation. These results are in accordance with previous data in the literature for another member of the FGFR family, showing that mouse embryonic fibroblasts transformed by EGFR overexpression display higher levels of FGFR4 expression than mouse embryonic fibroblasts transformed by other means.[30] FGFR1 overexpression in this context may further activate EGFR, which could confer a selective growth and tumorigenic advantage.

The EGFR-FGFR1 cooperation suggests a potential therapeutic opportunity for tumors with EGFR activation and high expression of these FGFRs. Indeed, we reported higher efficacy of dual EGFR/FGFR inhibition in EGFR-dependent models with FGFR1 overexpression in vitro and in vivo, showing dramatic results in EGFR-mutated cell line xenograft models overexpressing FGFR1 and in PDXs with high EGFR activation (one with an EGFR activating mutation and two with wild-type EGFR). Remarkably, two of these models, in which the combined EGFR/FGFR inhibition showed high efficacy, harbored the erlotinib resistance T790M mutation, which highlights the importance of the FGFR1-EGFR cooperation even in the presence of erlotinib resistance mutations. However, the high efficacy of this combined therapy in these two erlotinib-resistant models may be due to the relatively low duration of the treatments. In any case,

erlotinib-sensitive model (HCC827 xenograft). Four mice were included in the control and AZD4547 groups, and six mice were included in the EGFR inhibitor or combination treatment groups. AZD4547 was administered at a dose of 5 mg/kg/d in every case. (*C*) Western blots showing the impact of treatment of H1975 and HCC827 xenograft models with or without FGFR1 overexpression, on the activation of protumorigenic signaling. For the Western blots shown, three tumors coming from different mice were randomly selected In the FGFR1-overexpressing xenograft Western blots, one protein sample from the empty vector untreated control (EV) was added for comparison. *p* Values were obtained with the two-sided Mann-Whitney *U* test and are indicated by asterisks (*$p < 0.05$, **$p < 0.01$, and ***$p < 0.001$). pEGFR, phosphorylated EGFR; pSTAT3, phosphorylated signal transducer and activator of transcription 3; STAT3, signal transducer and activator of transcription 3; pAKT, phosphorylated AKT.

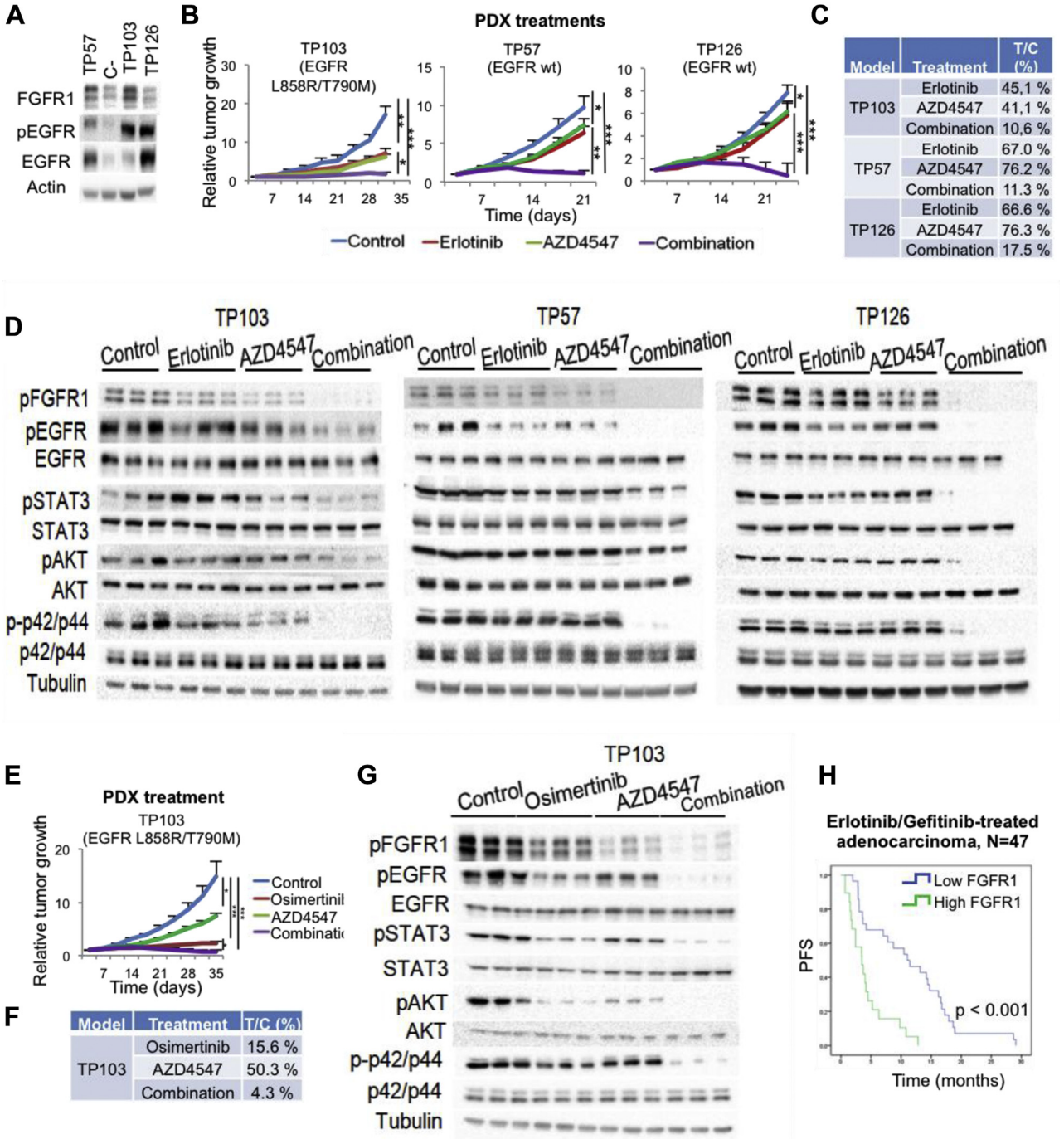

Figure 6. Effect of dual EGFR and fibroblast growth factor receptor inhibition in EGFR-activated fibroblast growth factor receptor 1 (FGFR1)-expressing lung adenocarcinoma patient-derived xenograft (PDX) models and impact of FGFR1 expression on response to anti-EGFR treatment. (*A*) Western blot showing the FGFR1, phosphorylated EGFR (pEGFR) and EGFR protein levels for the selected PDX models. The Western blot image was cropped and assembled from a broader image including more lanes. A negative control for pEGFR expression (control) in shown. (*B*) Effect of erlotinib and AZD4547 on tumor growth of lung adenocarcinoma PDX models. (*C*) Median relative size of treated tumor groups compared with that of the untreated tumor control group (T/C), expressed as percentages. (*D*) Western blots showing the impact of treatment on this model in the activation of protumorigenic signaling. (*E*) Effect of osimertinib and AZD4547 on tumor growth of the lung adenocarcinoma TP103 PDX model. (*F*) Median relative size of treated TP103 tumor groups compared with that of the untreated tumor control group (T/C), expressed as percentages. (*G*) Western blots showing the impact of osimertinib and AZD4547 treatment on the activation of protumorigenic signaling in the TP103 PDX model. (*H*) Effect of FGFR1 mRNA expression on progression-free survival of patients with erlotinib- or gefitinib-treated lung adenocarcinoma (see Supplementary Table 2 for a description of the cohort). FGFR1 mRNA expression was determined as stated in the Methods section, and beta-2-microglobulin housekeeping gene (*B2M*) expression was used to normalize FGFR1 expression across samples. To define the groups of

our results support the therapeutic potential of combined inhibition of EGFR and FGFR in EGFR-activated FGFR1-overexpressing tumors regardless of the presence of EGFR mutations. It is important to note that therapeutic regimens using more than one cell-signaling inhibitor frequently present increased adverse effects, which hinder their clinical application.[31,32] Toxicity enhancement is typically reported when unselective inhibitors that are molecularly promiscuous with numerous off-target effects are combined.[33,34] In this regard, a recent phase I trial testing the safety of erlotinib combined with the FGFR unselective inhibitor dovitinib in patients with NSCLC was terminated because of unacceptable toxicity.[35] In the present work, however, we have proposed combining EGFR inhibitors with a more selective FGFR1 inhibitor, hoping to result in a more favorable tolerability profile.

To assess whether the described cooperation between the EGFR and FGFR receptors was relevant at the clinical level, we determined the effect on progression-free survival of FGFR1 expression in patients with adenocarcinoma who were receiving erlotinib or gefitinib. As we had observed EGFR-FGFR1 cooperation taking place not only with mutated EGFR but also with its wild-type variant, we included wild-type and mutated EGFR tumors in this analysis and found shorter times to progression for patients with high FGFR1 expression. Interestingly, concordant results were obtained from analysis of an extended cohort in which all NSCLC histologic types were represented, which suggests that these findings may be applicable beyond adenocarcinoma tumors. In line with this, NSCLC cells from all histologic types with high FGFR1 expression levels and EGFR activation showed increased resistance to EGFR inhibitors. Upregulation of some FGFRs, such as FGFR1 or fibroblast growth factor receptor 2, and fibroblast growth factor receptor 3, mutations have been reported as mechanisms of acquired resistance to anti-EGFR therapy,[22–24,36,37] and combined EGFR and FGFR inhibition has been proposed in this setting. Furthermore, fibroblast growth factor receptor 2 inhibition has been linked to increased erlotinib sensitivity in several in vitro models of lung cancer.[38] These results certainly suggest a relationship between both EGFR and FGFR receptors in acquired resistance to anti-EGFR inhibition. However, we are the first to report a reciprocal activating interaction between FGFR1 and EGFR leading to intrinsic anti-EGFR resistance. Our data provide clinical evidence that tumors may exhibit high levels of FGFR1 expression before anti-EGFR therapy, which would make EGFR inhibition less effective: patients bearing tumors with these characteristics may benefit from dual inhibition of EGFR and FGFR, which would overcome this primary resistance.

Prooncogenic cooperation among receptor tyrosine kinases, similar to the FGFR1-EGFR interaction reported here for lung cancer, occurs in diverse malignancies. Insulin-like growth factor 1 receptor (IGF1R) has been found to interact with the insulin receptor in gastric and hepatocellular carcinoma cell lines, and the treatment of these cell lines with an antibody targeting this interaction reduces STAT3 and AKT activation.[39] In bladder cancer, it has been reported that EGFR can physically interact with platelet derived growth factor receptor beta and induce p42/p44 activation and resistance to anti-EGFR therapy.[40]

In the context of lung cancer, the heterodimerization of EGFR with IGF1R has also been described as a mechanism of erlotinib resistance, which could be bypassed through IGF1R inhibition.[41]

EGFR activation induces FGFR1 inhibition resistance in head and neck carcinoma cell lines, suggesting that the FGFR1-EGFR interaction may be of relevance in other tumor types as well.[42] To date, most targeted therapeutic approaches in the lung cancer setting have focused on concrete driver genetic alterations, but all of those data, along with the results of the present work, highlight the importance of a more comprehensive molecular characterization of tumors that harbor not just one but numerous molecular aberrations. The study of the coactivation of diverse signaling pathways may be of clinical relevance for predicting primary resistance to targeted therapies and the identification of efficacious combination therapies.

Thus, determination of the expression levels of FGFR1 and the activation of EGFR, not only in EGFR-mutated tumors but also in EGFR wild-type tumors, may be predictive of efficacy of EGFR inhibition, as well as of the effectiveness of combination therapy with EGFR

FGFR1-high and FGFR1-low patients, the median normalized FGFR1 mRNA expression value was used as cutoff. Four mice were included in the control and AZD4547 groups, and six mice were included in the EGFR inhibitor or combination treatment groups. Two different erlotinib concentrations were used for the PDXs experiments: 50 mg/kg/d for the erlotinib-resistant model (TP103) and 20 mg/kg/d for the models with no predicted erlotinib sensitivity (TP57 and TP126). Osimertinib was administered at a dose of 10 mg/kg/d. AZD4547 was administered at a dose of 5 mg/kg/d in every case. For the Western blots shown, three tumors coming from different mice were randomly selected. *p* Values for the in vivo assay were obtained with the two-sided Mann-Whitney *U* test and with the log-rank test for the survival analysis and are indicated by asterisks when not explicitly stated (*$p < 0.05$, **$p < 0.01$, and ***$p < 0.001$). Low/High FGFR1, low or high mRNA expression of FGFR1; pFGFR1, phosphorylated fibroblast growth factor receptor 1; pSTAT3, phosphorylated signal transducer and activator of transcription 3; STAT3, signal transducer and activator of transcription 3; pAKT, phosphorylated AKT.

and FGFR inhibitors. Therefore, we have proposed a highly effective therapeutic tailored approach for a subset of EGFR-dependent tumors with high FGFR1 expression levels, and we have provided molecular criteria for the selection of patients who would benefit from this therapy, thus extending the use of EGFR inhibitors to wild-type activated EGFR tumors.

Acknowledgments

Dr. Paz-Ares was funded by ISCIII (grants PI14/01964, PIE15/00076, PI17/00778 and DTS17/00089) and CIBERONC (CD16/12/00442) and cofunded by FEDER from Regional Development European Funds (European Union). Dr. Carnero was supported by grants from the Spanish Ministry of Economy and Competitiveness Plan Estatal de IþDþI 2013-2016, ISCIII (PI15/00045) and CIBERONC (CD16/12/00275) and cofunded by FEDER from Regional Development European Funds (European Union). Dr. Molina-Pinelo is funded by Ministry of Health and Social Welfare of Junta de Andalucía (PI-0046-2012, Nicolas Monardes Program C-0040-2016), Mutua Madrileña Foundation (2014) and ISCIII (PI17/00033). Dr. Ferrer is funded by AECC (AIO2015) and Ministry of Equality, Health and Social Policies of the Junta de Andalucía (PI-0029-2013), Comunidad de Madrid (B2017/BMD3884), and ISCIII (PI16/01311) and cofunded by FEDER from Regional Development European Funds (European Union). Dr. Quintanal-Villalonga is funded by ISCIII (FI12/00429). Dr. Ojeda-Márquez is funded by Ministry of Education, Culture and Sports (FPU13/02595). We thank those in the Spanish National Cancer Research Center Confocal Microscopy Unit for their specialized assistance and support. The authors thank the donors and the 12 de Octubre Hospital Biobank and University Hospital Virgen del Rocío Biobank for the human specimens used in this study.

Supplementary Data

Note: To access the supplementary material accompanying this article, visit the online version of the *Journal of Thoracic Oncology* at www.jto.org and at https://doi.org/10.1016/j.jtho.2018.12.021.

References

1. Moreira AL, Eng J. Personalized therapy for lung cancer. *Chest*. 2014;146:1649–1657.
2. Li S, Choi YL, Gong Z, et al. Comprehensive characterization of oncogenic drivers in Asian lung adenocarcinoma. *J Thorac Oncol*. 2016;11:2129–2140.
3. Hirsch FR, Scagliotti GV, Mulshine JL, et al. Lung cancer: current therapies and new targeted treatments. *Lancet*. 2017;389:299–311.
4. Inoue A, Yoshida K, Morita S, et al. Characteristics and overall survival of EGFR mutation-positive non-small cell lung cancer treated with EGFR tyrosine kinase inhibitors: a retrospective analysis for 1660 Japanese patients. *Jpn J Clin Oncol*. 2016;46:462–467.
5. Yu JY, Yu SF, Wang SH, et al. Clinical outcomes of EGFR-TKI treatment and genetic heterogeneity in lung adenocarcinoma patients with EGFR mutations on exons 19 and 21. *Chin J Cancer*. 2016;35:30.
6. Morgensztern D, Politi K, Herbst RS. EGFR mutations in non-small-cell lung cancer: find, divide, and conquer. *JAMA Oncol*. 2015;1:146–148.
7. Ahmad I, Iwata T, Leung HY. Mechanisms of FGFR-mediated carcinogenesis. *Biochim Biophys Acta*. 2012;1823:850–860.
8. Mellor HR. Targeted inhibition of the FGF19-FGFR4 pathway in hepatocellular carcinoma; translational safety considerations. *Liver Int*. 2014;34:e1–e9.
9. Penault-Llorca F, Bertucci F, Adelaide J, et al. Expression of FGF and FGF receptor genes in human breast cancer. *Int J Cancer*. 1995;61:170–176.
10. Feng S, Shao L, Yu W, Gavine P, Ittmann M. Targeting fibroblast growth factor receptor signaling inhibits prostate cancer progression. *Clin Cancer Res*. 2012;18:3880–3888.
11. Huang HP, Feng H, Qiao HB, Ren ZX, Zhu GD. The prognostic significance of fibroblast growth factor receptor 4 in non-small-cell lung cancer. *Onco Targets Ther*. 2015;8:1157–1164.
12. Jiang T, Gao G, Fan G, Li M, Zhou C. FGFR1 amplification in lung squamous cell carcinoma: a systematic review with meta-analysis. *Lung Cancer*. 2015;87:1–7.
13. Schildhaus HU, Nogova L, Wolf J, Buettner R. FGFR1 amplifications in squamous cell carcinomas of the lung: diagnostic and therapeutic implications. *Transl Lung Cancer Res*. 2013;2:92–100.
14. von Loga K, Kohlhaussen J, Burkhardt L, et al. FGFR1 amplification is often homogeneous and strongly linked to the squamous cell carcinoma subtype in esophageal carcinoma. *PloS One*. 2015;10:e0141867.
15. Weiss J, Sos ML, Seidel D, et al. Frequent and focal FGFR1 amplification associates with therapeutically tractable FGFR1 dependency in squamous cell lung cancer. *Sci Transl Med*. 2010;2:62ra93.
16. Paik PK, Shen R, Berger MF, et al. A phase Ib open-label multicenter study of AZD4547 in patients with advanced squamous cell lung cancers. *Clin Cancer Res*. 2017;23:5366–5373.
17. Perez-Moreno P, Brambilla E, Thomas R, Soria JC. Squamous cell carcinoma of the lung: molecular subtypes and therapeutic opportunities. *Clin Cancer Res*. 2012;18:2443–2451.
18. Seo AN, Jin Y, Lee HJ, et al. FGFR1 amplification is associated with poor prognosis and smoking in non-small-cell lung cancer. *Virchows Arch*. 2014;465:547–558.
19. Wynes MW, Hinz TK, Gao D, et al. FGFR1 mRNA and protein expression, not gene copy number, predict FGFR TKI sensitivity across all lung cancer histologies. *Clin Cancer Res*. 2014;20:3299–3309.
20. Goke F, Franzen A, Hinz TK, et al. FGFR1 expression levels predict BGJ398 sensitivity of FGFR1-dependent head and neck squamous cell cancers. *Clin Cancer Res*. 2015;21:4356–4364.

21. Chae YK, Ranganath K, Hammerman PS, et al. Inhibition of the fibroblast growth factor receptor (FGFR) pathway: the current landscape and barriers to clinical application. *Oncotarget*. 2017;8:16052–16074.
22. Azuma K, Kawahara A, Sonoda K, et al. FGFR1 activation is an escape mechanism in human lung cancer cells resistant to afatinib, a pan-EGFR family kinase inhibitor. *Oncotarget*. 2014;5:5908–5919.
23. Terai H, Soejima K, Yasuda H, et al. Activation of the FGF2-FGFR1 autocrine pathway: a novel mechanism of acquired resistance to gefitinib in NSCLC. *Mol Cancer Res. MCR*. 2013;11:759–767.
24. Ware KE, Hinz TK, Kleczko E, et al. A mechanism of resistance to gefitinib mediated by cellular reprogramming and the acquisition of an FGF2-FGFR1 autocrine growth loop. *Oncogenesis*. 2013;2:e39.
25. Guijarro MV, Leal JF, Blanco-Aparicio C, et al. MAP17 enhances the malignant behavior of tumor cells through ROS increase. *Carcinogenesis*. 2007;28:2096–2104.
26. Moneo V, Serelde BG, Blanco-Aparicio C, et al. Levels of active tyrosine kinase receptor determine the tumor response to Zalypsis. *BMC Cancer*. 2014;14:281.
27. Chou TC. Drug combination studies and their synergy quantification using the Chou-Talalay method. *Cancer Res*. 2010;70:440–446.
28. Ferrer I, Blanco-Aparicio C, Peregrina S, et al. Spinophilin acts as a tumor suppressor by regulating Rb phosphorylation. *Cell Cycle*. 2011;10:2751–2762.
29. McShane LM, Altman DG, Sauerbrei W, et al. REporting recommendations for tumor MARKer prognostic studies (REMARK). *Nat Clin Pract Urol*. 2005;2:416–422.
30. Seitzer N, Mayr T, Streit S, Ullrich A. A single nucleotide change in the mouse genome accelerates breast cancer progression. *Cancer Res*. 2010;70:802–812.
31. Padda S, Neal JW, Wakelee HA. MET inhibitors in combination with other therapies in non-small cell lung cancer. *Transl Lung Cancer Res*. 2012;1:238–253.
32. Giaccone G, Herbst RS, Manegold C, et al. Gefitinib in combination with gemcitabine and cisplatin in advanced non-small-cell lung cancer: a phase III trial–INTACT 1. *J Clin Oncol*. 2004;22:777–784.
33. Azad NS, Posadas EM, Kwitkowski VE, et al. Combination targeted therapy with sorafenib and bevacizumab results in enhanced toxicity and antitumor activity. *J Clin Oncol*. 2008;26:3709–3714.
34. Maione P, Gridelli C, Troiani T, Ciardiello F. Combining targeted therapies and drugs with multiple targets in the treatment of NSCLC. *Oncologist*. 2006;11:274–284.
35. Das M, Padda SK, Frymoyer A, et al. Dovitinib and erlotinib in patients with metastatic non-small cell lung cancer: a drug-drug interaction. *Lung Cancer*. 2015;89:280–286.
36. Crystal AS, Shaw AT, Sequist LV, et al. Patient-derived models of acquired resistance can identify effective drug combinations for cancer. *Science*. 2014;346:1480–1486.
37. Ware KE, Marshall ME, Heasley LR, et al. Rapidly acquired resistance to EGFR tyrosine kinase inhibitors in NSCLC cell lines through de-repression of FGFR2 and FGFR3 expression. *PloS One*. 2010;5:e14117.
38. Dai B, Yan S, Lara-Guerra H, et al. Exogenous restoration of TUSC2 expression induces responsiveness to erlotinib in wildtype epidermal growth factor receptor (EGFR) lung cancer cells through context specific pathways resulting in enhanced therapeutic efficacy. *PloS One*. 2015;10:e0123967.
39. Kim JG, Kang MJ, Yoon YK, et al. Heterodimerization of glycosylated insulin-like growth factor-1 receptors and insulin receptors in cancer cells sensitive to anti-IGF1R antibody. *PloS One*. 2012;7:e33322.
40. Black PC, Brown GA, Dinney CP, et al. Receptor heterodimerization: a new mechanism for platelet-derived growth factor induced resistance to anti-epidermal growth factor receptor therapy for bladder cancer. *J Urol*. 2011;185:693–700.
41. Morgillo F, Woo JK, Kim ES, Hong WK, Lee HY. Heterodimerization of insulin-like growth factor receptor/epidermal growth factor receptor and induction of survivin expression counteract the antitumor action of erlotinib. *Cancer Res*. 2006;66:10100–10111.
42. Koole K, Brunen D, van Kempen PM, et al. FGFR1 is a potential prognostic biomarker and therapeutic target in head and neck squamous cell carcinoma. *Clin Cancer Res*. 2016;22:3884–3893.